Performance Comparisons of Cooperative and Adaptive Cruise Control Testing

A&WMA's 113th Annual Conference & Exhibition
June 29 - July 2, 2020

Paper # 781164

Andrew C. Eilbert, Anne-Marie Chouinard, Tim A. Tiernan, and Scott B. Smith
Volpe National Transportation Systems Center
U.S. Department of Transportation
55 Broadway
Cambridge, MA 02142

ABSTRACT

A burgeoning field of research has begun to directly compare the impacts of pairing vehicle automation and connectivity to automation alone. While most recent impact studies that evaluate adaptive cruise control (ACC) and cooperative adaptive cruise control (CACC) rely on traffic simulation, the US Department of Transportation has recently conducted ACC and CACC tests on a closed-loop track with and without vehicle-to-vehicle communications (V2V).

The Cooperative Automated Research Mobility Applications (CARMA) multi-year testing program has studied five passenger vehicles equipped with production ACC technology and more recently with CACC technology featuring dedicated short-range communication (DSRC) systems. These tests were run at the Aberdeen Proving Ground utilizing similar conditions and drive schedules.

We compared the performance of these ACC and CACC runs by examining vehicle trajectory data and assessing any operational and environmental impacts. Our findings confirm earlier modeling studies that indicate a platoon of CACC-enabled vehicles will often stabilize fluctuations in speed and the following time gap between vehicles. Given some limitations in CARMA data quality and in the use of operating modes to calculate tailpipe emissions and fuel consumption, we could not draw definite conclusions on emissions or energy impacts. These results also suggest that, depending on the configuration of the ACC and CACC controls, there may be tradeoffs between improved traffic flow, user comfort, and environmental benefits.

INTRODUCTION

Vehicle automation and connectivity are expected to revolutionize the future of transportation. Many studies have modeled the benefits of connected and automated vehicles, but far fewer have investigated the incremental impact of pairing V2V communications with an automated driving system such as adaptive cruise control (ACC). Fewer still have attempted to measure the performance of driving with cooperative adaptive cruise control (CACC) (*1*), and very few have explicitly compared the performance

of ACC and CACC. Comparisons of ACC and CACC systems through rigorous instrumented vehicle tests are needed to determine any advantages of cooperative automation over automation without communications.

Connected and automated vehicles (CAVs) have several sometimes competing, sometimes synergistic impacts:

- Traffic flow and operations,
- Safety and user comfort, and
- Energy consumption and emissions.

While it may be possible to achieve optimal benefits for any one or perhaps two of these impact areas, a multi-criteria optimization often leads to certain tradeoffs (*2*). For example, a CACC system may be able to improve roadway capacity by decreasing the following time gaps between vehicles but not without some consequences. The shorter time gaps may also create a less smooth driving trace, pose a greater risk to user safety, and increase energy consumption and emissions. This paper explores potential tradeoffs of these three impact areas under live test conditions with an emphasis on finding a suitable middle ground for operational and environmental benefits. Safety measures are critically important to the viability of ACC and CACC technologies, but we did not consider them directly in this study.

One of the few studies that has tested both ACC and CACC driving under similar conditions is the US Department of Transportation's Cooperative Automation Research Mobility Applications (CARMA) Program. Since 2014, Turner-Fairbank Highway Research Center (TFHRC) has been testing passenger vehicles with range sensors for ACC-following, sometimes coupled with dedicated short range communications (DSRC) on a 4.5-mile closed loop at the Aberdeen Proving Ground in Maryland (*3*). An aerial image of the test track from a recent CARMA report is reproduced in Figure 1a (*4*). This study makes use of vehicle test data collected through CARMA to evaluate benefits and tradeoffs in terms of operations and environmental impacts.

Instrumented Vehicle Testing

As part of the CARMA Program, FHWA purchased five Cadillac SRX vehicles from model year 2013, each equipped with ACC technology from the original equipment manufacturer (OEM), see image of instrumented vehicles in Figure 1b (*3*). The SRXs were then retrofit with third-party DSRC devices by TFHRC engineers and technicians to demonstrate CACC as a proof-of-concept (*4*). While much of the early CARMA testing at Aberdeen had been to evaluate CACC functionality, there were some initial test runs with the production ACC system as a baseline. More recent tests have refined CACC platooning and following algorithms (*5*). The All Predecessor Following (APF) platooning algorithm was developed and programmed by FHWA, such that a platoon forms behind the lead vehicle and the following vehicles utilize V2V communications to maintain an appropriate following time gap between not just the preceding vehicle but all other vehicles in the platoon (*6*). Current CARMA testing is implementing SAE Level 2 of automation capabilities (*7*), cooperative lane change and merging, and now public road applications. Most of the sensors on the instrumented CARMA vehicles recorded at 10 Hz, though a few had 20 Hz measurements.

Figure 1. (a) Aerial representation of the Aberdeen Proving Ground with labeled test track waypoints, and (b) image of the five instrumented Cadillac SRXs for CARMA testing (*3*, *4*).

(a) 

(b) 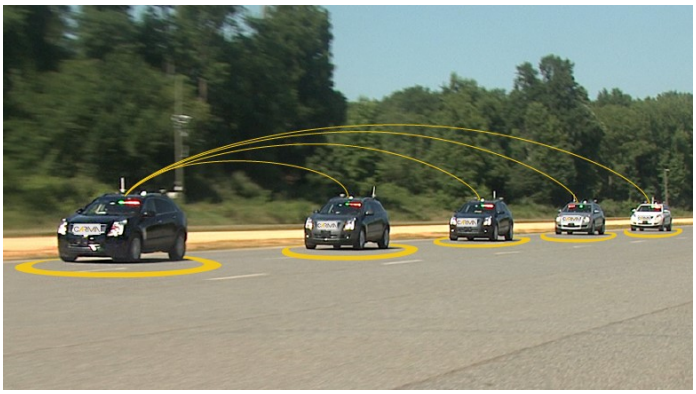

To date, there have been three testing phases: CARMA1 (2014-2016), CARMA2 (2016-2018), and CARMA3 (2018-present, expected to finish later in 2020). For this analysis, two ACC runs in July 2016 were selected from CARMA1 and six CACC with APF runs in July 2018 were selected from CARMA2 for comparison. While the CARMA1 ACC test vehicles utilized the production algorithm for vehicle following, any references to CACC later in this paper assume that the CARMA2 CACC test vehicles are operating with the APF platooning algorithm. Both CARMA1 and CARMA2 were performed with similar driving traces and platoon formations. For reference, both CARMA datasets are publicly available through the Intelligent Transportation Systems DataHub (*7*, *8*).

Literature Review

In a previous systematic review and meta-analysis examining the operational and environmental impacts of ACC and CACC studies, we identified some related testing (*8*). However, many of these research studies utilized heavy-duty trucks or had been conducted at signalized intersections and are therefore not directly comparable to CARMA. Relevant ACC and CACC testing over the past decade has primarily been completed by TFHRC and other research offices at FHWA, the California Partners for Advanced Transit and Highways (PATH), and researchers from Dutch universities.

Bu, Tan, and Huang were able to integrate a custom CACC controller with the commercially available ACC and were one of the first to show the shorter time gap for CACC than a human driver (*9*). Similarly, Nowakowski et al. researched the willingness of drivers to accept various time gaps, finding that CACC driving could lead to shorter gaps than either ACC or naturalistic driving (*10*). Both studies show that V2V communications can lead to closer following behavior for a CACC platoon than an ACC platoon and subsequently greater highway capacity. Recent studies by Milanés and others at California PATH have tested mixed traffic scenarios and tried to validate an ACC driver model against experimental data (*11*, *12*). This research from California has been focused on investigating CACC dynamics and controls more so than potential fuel savings and emission benefits. Ploeg from TNO Eindhoven and van Arem from TU Delft have also elaborated on controller design and model development for these cooperative automation systems (*13*, *14*).

There is a growing body of simulation studies suggesting that CACC and to some extent ACC will smooth driving and reduce energy consumption and emissions compared to manual drivers (*15–18*), but there is limited empirical evidence to confirm these environmental benefits. The CARMA Program was intended to fill some of those data collection gaps. Elsewhere, Ma et al. has shown some moderate fuel efficiency gains during field tests of light-duty CAVs, up to more than 20% fuel savings on a particular

hilly arterial segment (*19*). Intuitively, Knoop et al. finds that string instability of an ACC platoon causes greater fuel consumption and user discomfort (*20*). Further ACC and CACC testing is needed to validate fuel use and emission reductions.

The most recent experiments with CACC-enabled vehicles are reporting promising energy and emission results. For light-duty CACC applications coupled with signal coordination, Liu et al. has found fuel efficiency improves by more than 30% in a scenario with 40% CACC market penetration (*21*). For heavy-duty applications, Ramezani et al. reported significant fuel savings for CACC truck platoons using a new regression model for aerodynamic drag developed with the latest experimental data (*22*). This paper proposes to compare emissions and fuel use for production ACC-following and CACC with APF applications.

STUDY DESIGN

The first step in processing the instrumented vehicle data from Aberdeen was to combine the two ACC runs (1546 and 1558) in CARMA1 and the six CACC runs (5, 6, 9, 10, 12, and 13) in CARMA2 into a single, unified dataset for this performance evaluation. All the ACC and CACC runs used the same general test procedure (5.0.5) of alternating 45-mph and 60-mph cruising periods, but there were some clear differences in the recorded driving traces. This unified CARMA dataset was cleaned and parsed for better comparability between runs and then additional calculations were made to evaluate operational and environmental performance. The methodology for preparing and executing these calculations of performance measures and their results are described in the sections below.

All the runs in CARMA1 and CARMA2 deployed five instrumented vehicles and referred to each vehicle in the platoon by its color. The black vehicle served as the lead vehicle for all the runs except one. Each run had a distinct vehicle order with many of the CACC runs having the same order. For the ACC runs from CARMA1 (*4*), the vehicle order was as follows:

- 1546: black, green, silver, grey, and white
- 1558: black, white, grey, black, and green

Respectively, for the CACC runs from CARMA2 (19), the vehicle order was as follows:

- 5: black, green, grey, silver, and white
- 6: black, green, grey, silver, and white
- 9: black, green, grey, silver, and white
- 10: black, green, grey, silver, and white
- 12: white, silver, grey, black, and green
- 13: black, green, grey, silver, and white

Given the varying vehicle color order for each run, the lead vehicle and every subsequent following vehicle was labeled as LV, FV1, FV2, FV3, and FV4 for consistency and comparability. Note that ACC Run 1546 and CACC Run 5, 6, 12, and 13 were single-loop test applications, while ACC Run 1558 and CACC Run 9 and 10 were two-loop applications.

Processing of Instrumented Vehicle Data

The following common fields collected from CARMA1 and CARMA2 were used to generate the initial unified test dataset, including raw variable labels where appropriate:

- run number,
- UTC time,
- elapsed time of run in seconds,
- vehicle color (how the five vehicles were uniquely identified in each run),
- speed from the vehicle's controller area network (CAN) bus in meters per second [*vehspdavgdrvn_srx*],
- secondary speed from an aftermarket global positioning system (GPS) device in meters per second [*velocity_fwd_pinpoint*],
- distance to preceding vehicle in meters from forward-looking radar sensors for vehicle range measurements [*flrrtrk1range_srx* for CACC and *distToPVeh* for ACC],
- axle torque in Newton-meters [*acc_axle_torque_cmd_axle_torque_request*], and
- angular speed of engine in revolutions per minute (RPM)[*engine_rpm_srx*].

The CACC APF platooning algorithm in CARMA2 used the pinpoint GPS location to measure and control the headway between the GPS antenna on the lead vehicle and on the following vehicles. For the ACC runs, the white vehicle was missing CAN bus speed, torque, and RPM data, so we utilized the GPS speed readings as necessary and removed all the dependent measures from the white vehicle. All other vehicle speeds were recorded directly from the vehicle CAN bus according to the average speeds of measured non-propulsive wheels.

We converted speed to miles per hour (mph) and applied some additional constraints to the full dataset to cut out some initial idling and ramp-up time: 1) records prior to the lead vehicle first reaching 20 mph were removed, 2) records after the lead vehicle then dropped below 19 mph were also removed, and finally 3) any other records with null values in speed data were removed as well. We elected not to cut the tail of CACC Run 9 since the lead vehicle did not drop below 19 mph before the end of recording. Further calculations were then performed on the combined ACC and CACC dataset to compare the operational impacts.

RESULTS AND DISCUSSION

This paper has broken results into two subsections: one for vehicle operations and the other for emissions and energy use impacts. In this section, we discuss the operational and environmental data and then any calculations made to present results.

Operational Data and Calculations

While acceleration was measured onboard the test vehicles, it also had noticeable data gaps as well. We calculated acceleration a (in feet per second squared) as the change in speed v over the change in time elapsed t between the current time step i and the previous step $i-1$ instead of having an incomplete range of acceleration data and potential inconsistencies between measured speed and acceleration.

Similarly, vehicle jerk is the second derivative of measured speed and serves as a proxy for user comfort (*23*). Jerk j was calculated (in feet per second cubed) as the change in derived acceleration over the change in time elapsed between the current time step and the previous step.

For each time step, the following time gap (reported in seconds) is the time needed to travel between the lead vehicle's rear bumper and the following vehicle's front bumper at the instantaneous speed of the following vehicle (*24*). Finally, we calculated the change in distance traveled for the lead vehicle of every run as the CAN bus speed multiplied by the change in time elapsed over consecutive time steps.

For some preliminary comparisons, the mean values of speed, time gap, and distance traveled in Table 1 for every run, where the five-vehicle platoon was considered except for the distance traveled, which was only for the lead vehicle.

Table 1. Summary statistics of the performance measures across ACC and CACC runs (all vehicles were included in averages, but only the distance traveled of the lead vehicle was reported).

	Average Speed (mph)	*Average Time Gap (s)*	*Distance Traveled (mi)*
Run No.	**Full Platoon**		**LV Only**
CACC 5	49.99	1.010	3.685
CACC 6	49.12	0.933	3.984
CACC 9	53.84	0.919	8.154
CACC 10	53.88	0.666	8.874
CACC 12	49.83	0.886	3.714
CACC 13	49.97	1.325	3.638
ACC 1546	52.35	0.886	4.320
ACC 1558	53.13	0.876	8.804

There is little to no difference in the average speed and time gap between the ACC and CACC runs. These summary statistics are a helpful reference but do not demonstrate differences in ACC and CACC driving behavior. As we found in the meta-analysis of ACC and CACC studies, time gaps consistently shorter than one second can be maintained safely by human drivers on congested highways, so it appears the CARMA platoons could have achieved even shorter gaps. While CACC should be able of achieving shorter gaps, the measured gap ultimately depends on where the target gap is set and how well the following technology can meet the target. For example, the test vehicles in CACC Run 10 did reasonably well at achieving the relatively short target of 0.6 s, but the gap realized was a bit longer than desired. Nonetheless, many of the other CACC runs had target gaps upwards of 0.6 s, similar to the targets for the ACC runs. In real-world mixed traffic, many drivers operating with ACC find gaps of less than 1.0 s are necessary to discourage others from cutting in (*8*).

To further compare the performance differences of the ACC and CACC runs, we have plotted the time series of speed, jerk, and time gap. Jerk was chosen over acceleration in these comparisons because the trends were similar and jerk reflected starker differences between ACC and CACC behavior. Each run was indexed when it began recording and the speed-based constraints above were then applied based on the start and end time cutpoints. The ACC sensors are designed to follow the directly preceding vehicle while the DSRC devices on the CACC-enabled vehicles can communicate with all other vehicles in the platoon. The controller design and the use of communicated data account for the ACC and CACC behavior differences.

When examining the speed traces across all the runs in Figure 2a, it becomes evident that ACC platoons behave differently than the CACC platoons. The ACC-following vehicles oscillate after acceleration and deceleration and take some time to match the cruising speed of the lead vehicle. It is particularly apparent during braking events for both ACC runs. This undershooting behavior while braking is most pronounced in ACC Run 1546 but also occurs in Run 1558. In contrast, the CACC runs show tight following and have minimal oscillations when accelerating or braking. Even with minor latency in CACC-following, it does not oscillate like ACC-following.

Figure 2. (a) Time series of the vehicle speed readings (mph) from the CAN bus for the five instrumented SRXs in each run.

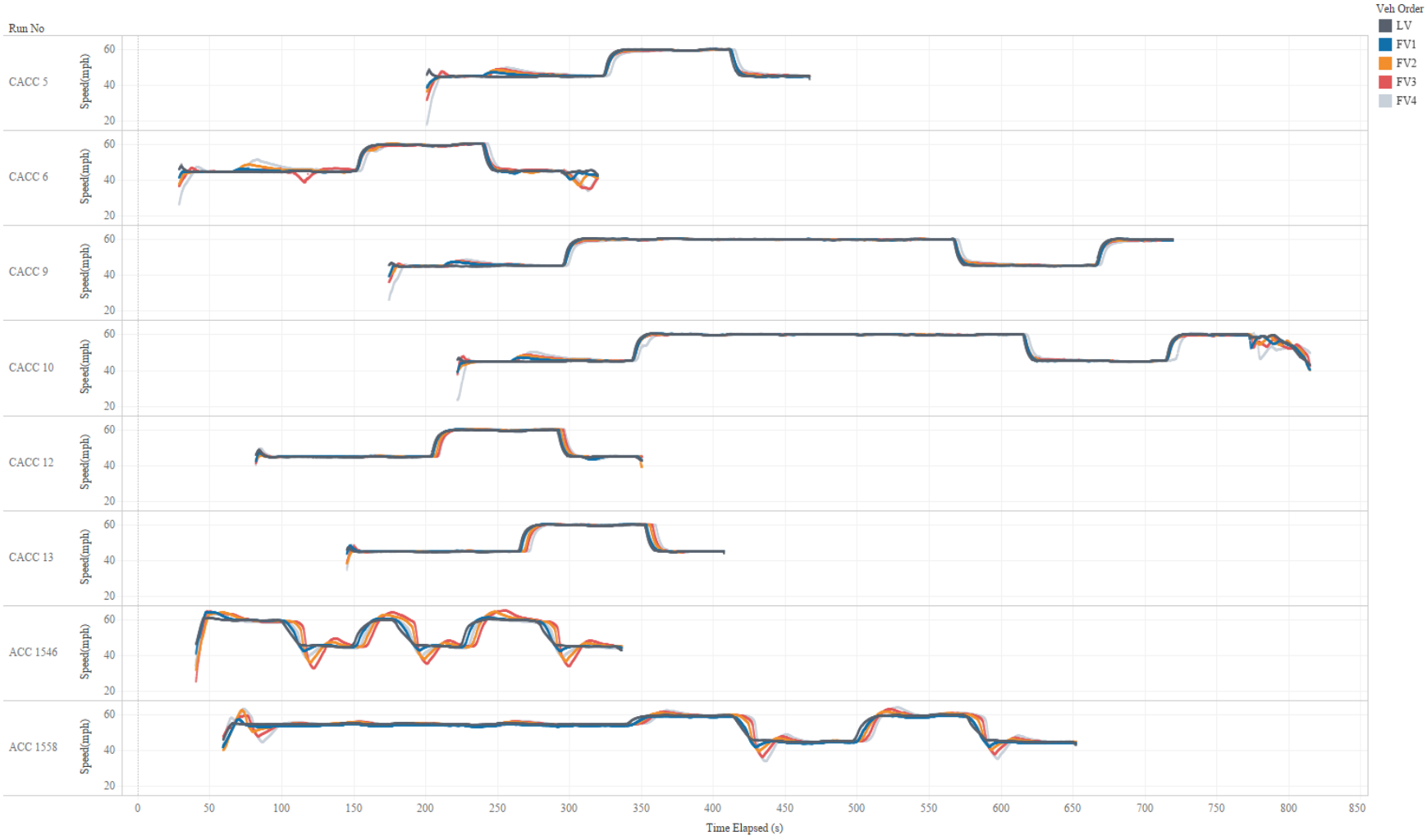

Figure 2. (b) Time series of the calculated vehicle jerk (ft/s^3) for the five instrumented SRXs in each run.

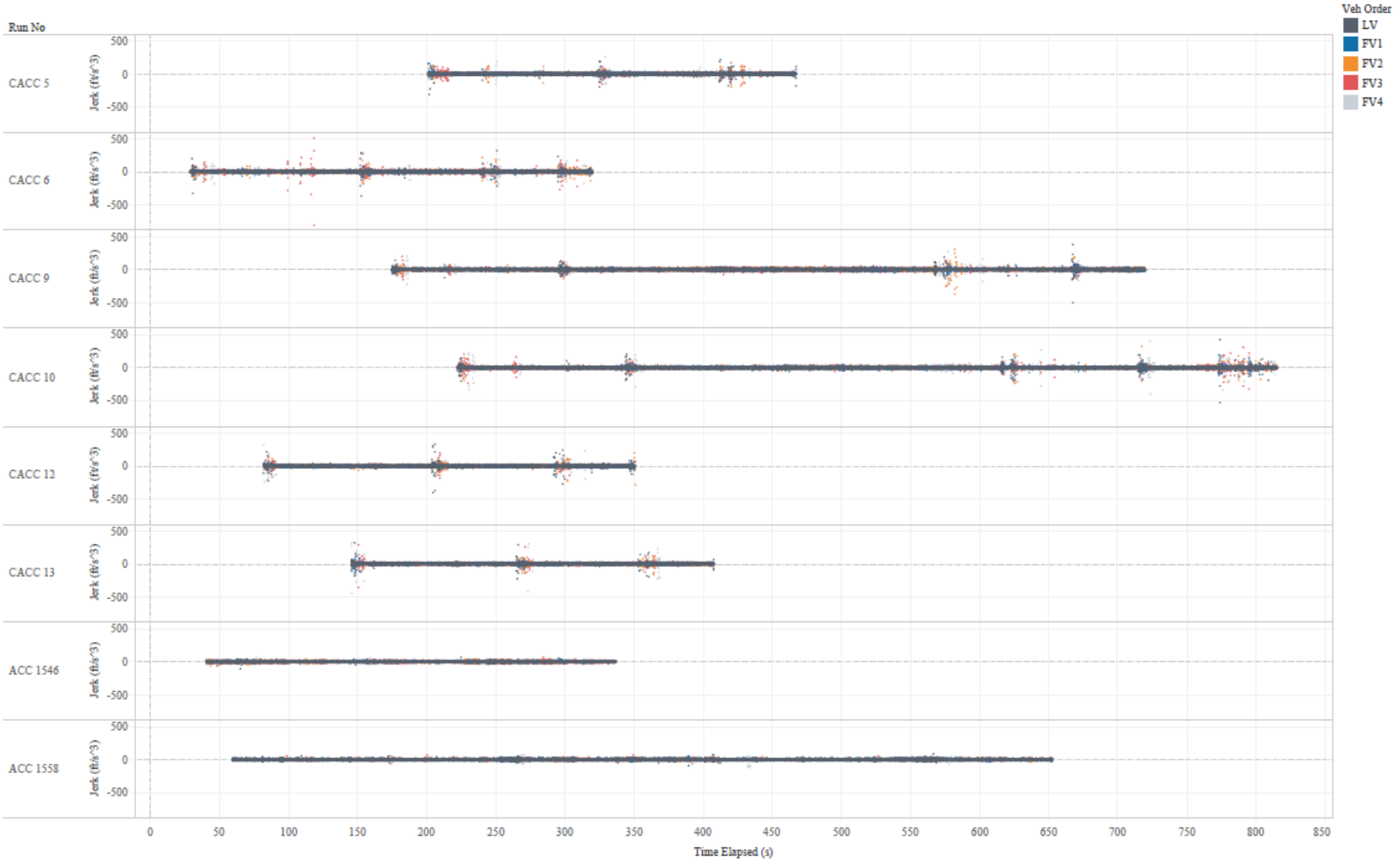

Figure 2. (c) Time series of the following time gap (s) to the preceding vehicle for the five instrumented SRXs in each run.

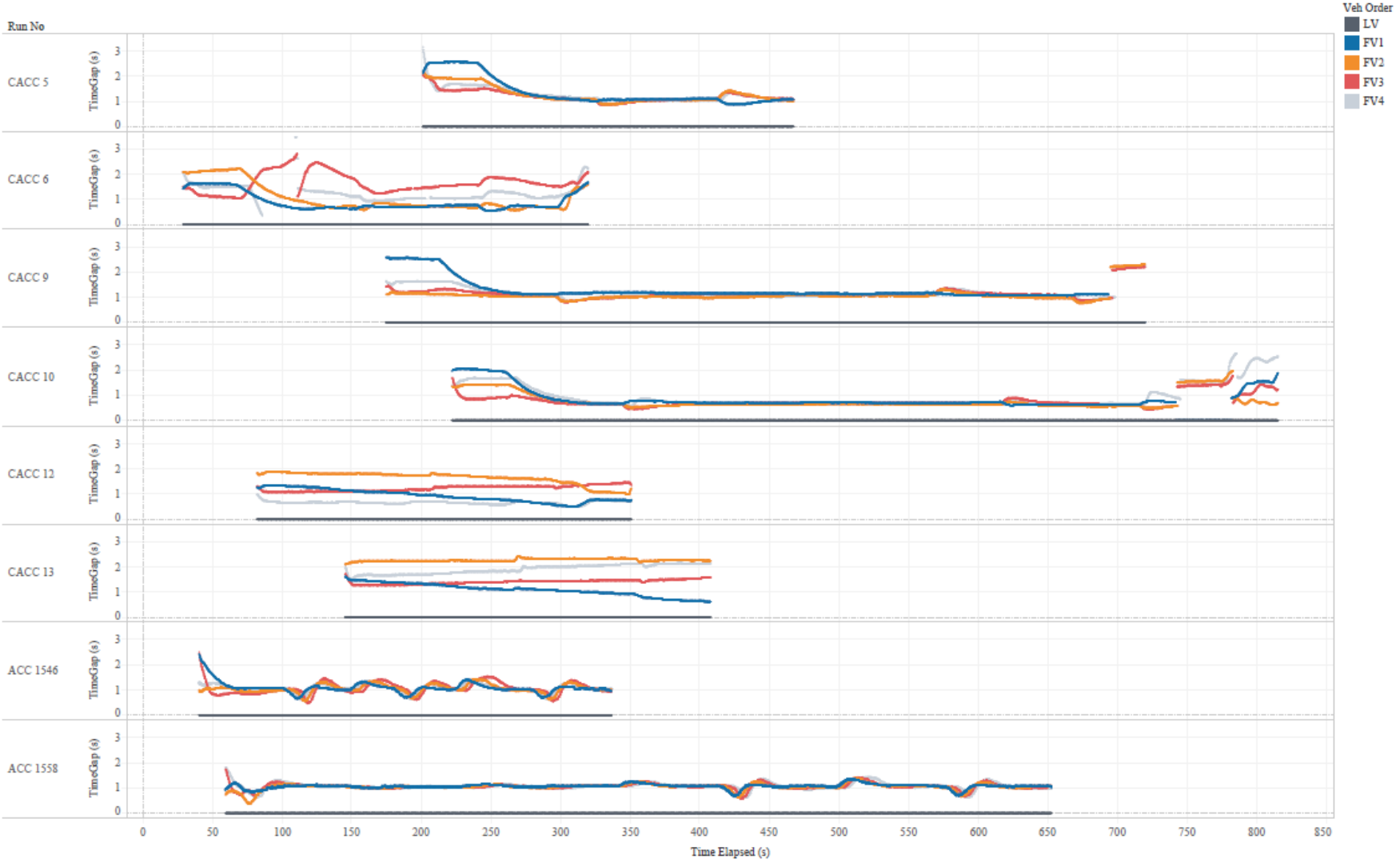

The time series of jerk in Figure 2b also draws a distinction between ACC and CACC behavior. The CACC runs have some moments of intense jerk during acceleration and braking events. This jerky behavior in CACC-following is characterized by scatter at specific acceleration/deceleration transition points in the driving traces, whereas ACC-following does not show much scatter. Upon closer inspection, the maximum absolute values of calculated jerk for the CACC runs was in the range of 300-500 ft/s^3, while for the ACC runs was 70-120 ft/s^3. These are likely to be sensor or signal errors and generate unrealistic values; however, these outliers were indicative of sudden changes in acceleration and therefore not discarded from the time series for jerk.

All the test vehicles were operated by professional drivers willing to accept a time gap setting of about one second. Despite having similar one-second gaps, the ACC and CACC platoons show different trends in Figure 2c. The ACC-following vehicles fluctuate around one-second gaps, never achieving very stable gaps. In comparison, the CACC-following vehicles converge to time gaps of roughly one second and demonstrate much greater string stability, particularly for CACC Runs 5, 9, and 10. In these highlighted runs, even when the vehicles are accelerating or braking, the CACC systems hold consistent gaps. We presume that CACC Runs 12 and 13 do not converge due to differences in the CACC APF controller configurations, which may have had varying gap settings. The discontinuities in the time gap plot, particularly for CACC Runs 9 and 10, seem to occur primarily at the end of testing when the platoon is breaking up and dispersing, although the data was still being collected. Discontinuities could also be an artifact of the removed null values. Nevertheless, the CACC runs have tighter following behavior than the ACC runs, but that seems to have some tradeoffs in terms of driving smoothness, user comfort, and environmental benefits.

We also evaluated the comparability of ACC and CACC runs. Since each run had differing cruise durations at 45 and 60 mph and a differing number of transitions, we utilized the kinetic intensity ratio (reported as km^{-1}) described by O'Keefe et al. to determine an index for the relative energy consumption by run (*25*). The KI ratio is defined as the characteristic acceleration $\tilde{a}$ over the aerodynamic speed squared v_{aero}^2 for the current time step i and the previous step $i-1$, as expressed in Equation 1. As the longer form given in Equation 2, it becomes

$$KI = \frac{\tilde{a}}{v_{aero}^2}, \tag{1}$$

$$KI \cong \frac{\sum_{i=1}^{N-1} positive\left(\frac{1}{2}(v_i^2 + v_{i-1}^2) + g \cdot \Delta h_{i,i-1}\right)}{\sum_{i=1}^{N-1} \overline{v_{i,i-1}^3} \cdot \Delta t_{i,i-1}} \cong \frac{\sum_{i=1}^{N-1} positive\left(\frac{1}{2}(v_i^2 + v_{i-1}^2)\right)}{\sum_{i=1}^{N-1} \overline{v_{i,i-1}^3} \cdot \Delta t_{i,i-1}}, \tag{2}$$

where for CARMA the measured CAN bus speed v and time elapsed t were used and the second numerator term with acceleration due to gravity g and elevation h drops because the Aberdeen closed-loop tests are assumed to be at zero grade or near-zero grade. The lead vehicle's KI ratio is a decent representation of the run's overall KI ratio, as shown in Figure 3a and Figure 3b respectively, in order to understand the relative energy expended by run.

There is some notable variability in kinetic intensity between the runs. We observe that the longer, less dynamic runs, namely CACC Runs 9 and 10 as well as ACC Run 1558, have lower KI ratios. Additionally, the later following vehicles appear to have larger KI ratios, but it is difficult to make any conclusions about the KI ratios for ACC compared to CACC. There may be a need to better synchronize the kinetic intensity across runs in future testing and analysis.

Figure 3. Kinetic intensity ratios by run for (a) lead vehicles and (b) all five vehicles in platoon.

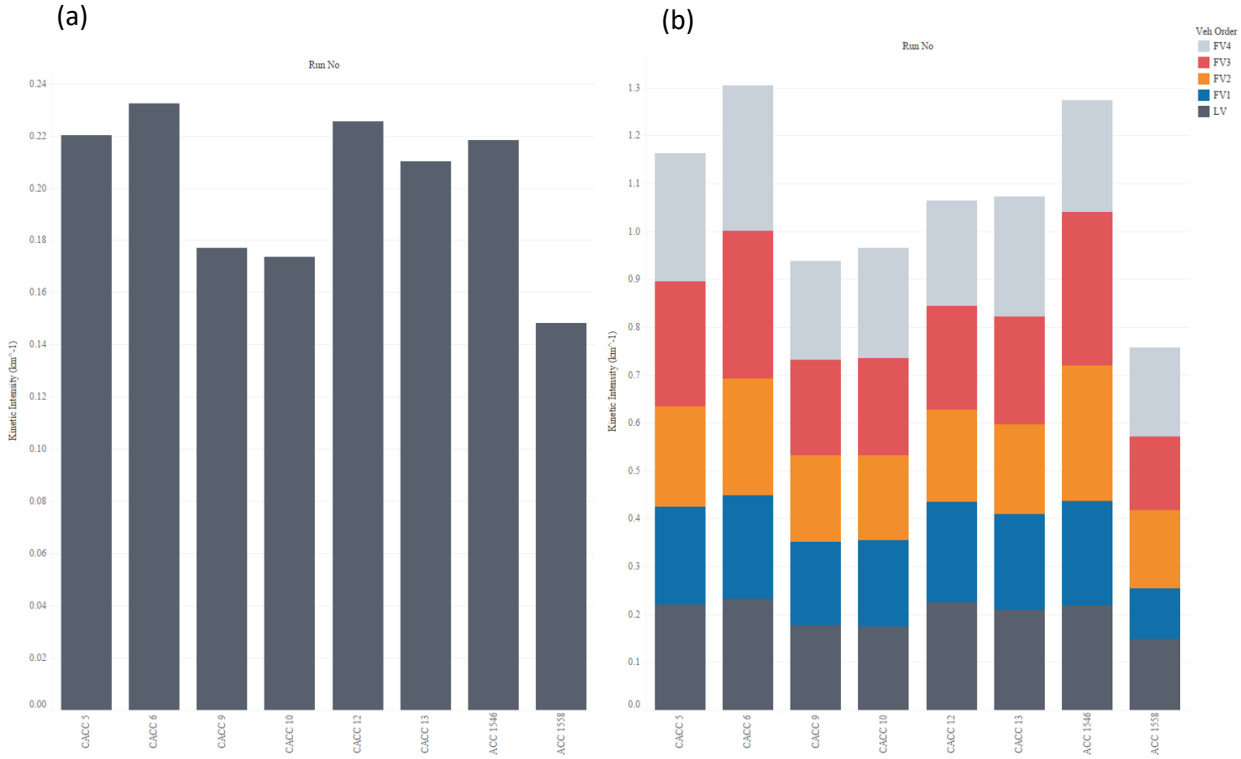

Environmental Data and Calculations

In some scenarios, tighter following behavior comes at the detriment of environmental benefits, particularly fuel savings and emissions reductions. The CARMA test vehicles were not instrumented with any emissions monitoring equipment and some of the runs measured fuel consumption while others did not, so an energy and emissions model was needed. We chose the latest EPA's Motor Vehicle Emission Simulator (MOVES2014b) to estimate modal, project-level tailpipe emissions and fuel use based on the vehicle-specific power (VSP), speed, and acceleration (*26*). More commonly, VSP is calculated from the speed and acceleration using either test data or microscopic traffic simulation results, although VSP for the current time step i can also be calculated from axle torque τ and RPM number n_{RPM} if collected and available. These two VSP calculation methods are described below. The speed and acceleration derivation of $VSP(v, a)$ is Equation 3 and the torque and RPM derivation of $VSP(\tau, RPM)$ is Equation 4.

$$VSP(v,a)_i = \frac{Av_i + Bv_i^2 + Cv_i^3 + mv_i a_i}{m}, \quad \textbf{(3)}$$

where A is the tire rolling resistance coefficient, B is the rotational resistance coefficient, C is the aerodynamic drag coefficient, and m is the vehicle mass. Default road load coefficients A, B, and C for a sports utility vehicle (MOVES sourceTypeID 31) came from the sourceusetypephysics table in the MOVES2014b database. We pulled the vehicle mass m for the Cadillac SRX from the listed OEM curb weight (*27*), such that

- A = 0.22112 kW-s/m (kilowatts-seconds per meter),
- B = 0.00283757 kW-s/m^2 (kilowatts-seconds per meter squared),
- C = 0.000698282 kW-s/m^3 (kilowatts-seconds per meter cubed), and
- m = 1.940 metric tons.

To use the road load coefficients as listed above, speed and acceleration must be in SI units, m/s and m/s^2 respectively. Even though the speed is directly measured, this VSP calculation method relies heavily on approximations of vehicle loads and driving behavior, whereas the alternative VSP method with torque and RPM is based on specific high-resolution measurements (*28*). This alternative VSP can be computed through Equation 4:

$$VSP(\tau, RPM)_i = \frac{\pi}{30 \times 10^3}\left(\frac{\tau \cdot n_{RPM}}{m}\right), \quad \textbf{(4)}$$

where the 10^3 factor is for converting watts to kilowatts. The two VSP methods yield starkly different results and these differences are evident regardless of whether considering an ACC or a CACC run. Figure 4 shows that the reference $VSP(v, a)$ has much more noise than the alternative $VSP(\tau, RPM)$ for the lead vehicle in both CACC Run 9 and ACC Run 1558. Both VSP methods produced a couple of unrealistic spikes, particularly $VSP(\tau, RPM)$, which yielded some outlier data.

Figure 4. Time series of reference $VSP(v, a)$ (top) and alternative $VSP(\tau, RPM)$ (bottom) for lead vehicle in representative runs CACC 9 and ACC 1558 (some peaks truncated to highlight noise).

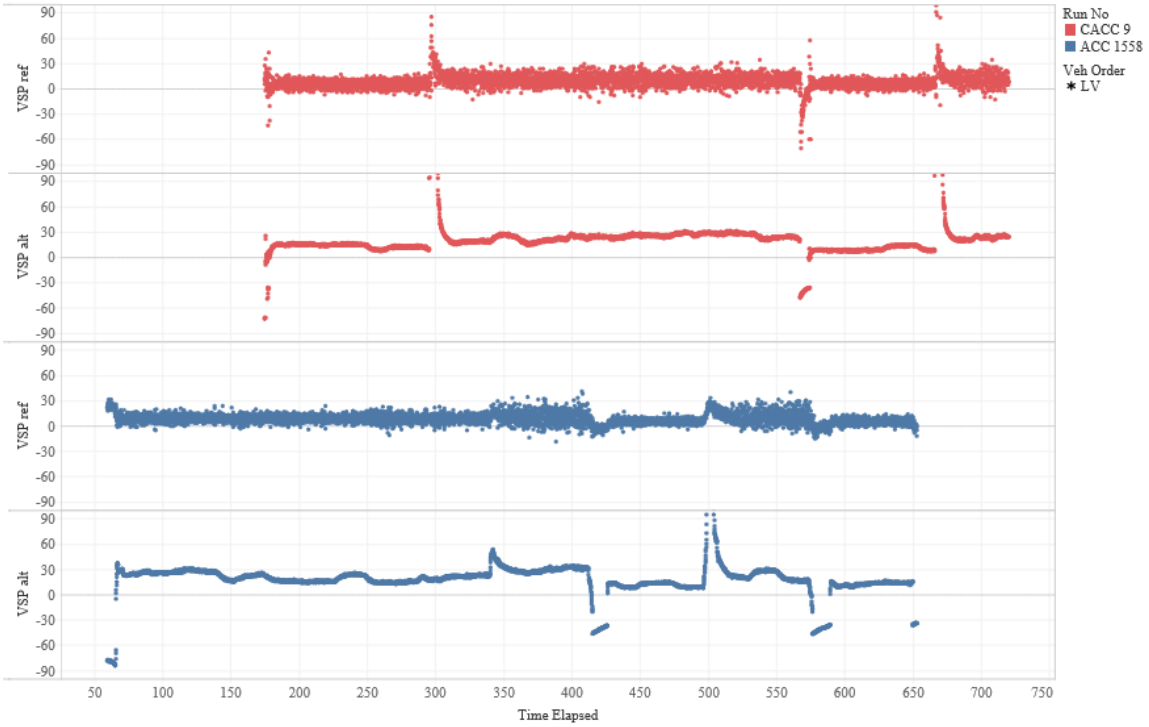

In CACC Run 9, for instance, the maximum $VSP(v,a)$ value is nearly 90 kW/metric ton, roughly 2-3 times greater than the threshold for the highest MOVES VSP bin, while the maximum $VSP(\tau,RPM)$ value reaches 330-350 kW/metric ton, about 11-12 times greater than the highest MOVES bin. Even so, the persistent noise in $VSP(v,a)$ makes it less suitable for emissions and energy modeling than $VSP(\tau,RPM)$ when considering the rare extreme outliers.

These differences in power demand carry through to the MOVES operating mode distributions, which are dependent on vehicle speed, acceleration, and VSP and which form the basis of any project-level energy and emissions estimates. The operating modes were assigned by the conditions for the three performance measures laid out below in Table 2. MOVES operating mode assignments based on VSP, speed, and acceleration for each time step *i* that we have reproduced from the MOVES technical documentation of light-duty emission rates (*29*). After each time step across all runs is assigned an operating mode, the ACC and CACC driving traces were aggregated into distributions by time spent in each operating mode by run. These operating mode distributions provide helpful illustrations of how ACC and CACC behavior differed.

Table 2. MOVES operating mode assignments based on VSP, speed, and acceleration for each time step *i*

Operating Mode (opModeID)	Operation Mode Description	Vehicle-Specific Power (VSP_i, kW/metric ton)	Vehicle Speed (v_i, mph)	Vehicle Acceleration (a_i, mph/s)
0	Deceleration/Braking			$a_i \le -2$ OR ($a_i < -1$ AND $a_{i-1} < -1$ AND $a_{i-2} < -1$)
1	Idle		$-1 \le v_i < 1$	
11	Coast	$VSP_i < 0$	$1 \le v_i < 25$	
12	Cruise/Acceleration	$0 \le VSP_i < 3$	$1 \le v_i < 25$	
13	Cruise/Acceleration	$3 \le VSP_i < 6$	$1 \le v_i < 25$	
14	Cruise/Acceleration	$6 \le VSP_i < 9$	$1 \le v_i < 25$	
15	Cruise/Acceleration	$9 \le VSP_i < 12$	$1 \le v_i < 25$	
16	Cruise/Acceleration	$12 \le VSP_i$	$1 \le v_i < 25$	
21	Coast	$VSP_i < 0$	$25 \le v_i < 50$	
22	Cruise/Acceleration	$0 \le VSP_i < 3$	$25 \le v_i < 50$	
23	Cruise/Acceleration	$3 \le VSP_i < 6$	$25 \le v_i < 50$	
24	Cruise/Acceleration	$6 \le VSP_i < 9$	$25 \le v_i < 50$	
25	Cruise/Acceleration	$9 \le VSP_i < 12$	$25 \le v_i < 50$	
27	Cruise/Acceleration	$12 \le VSP_i < 18$	$25 \le v_i < 50$	
28	Cruise/Acceleration	$18 \le VSP_i < 24$	$25 \le v_i < 50$	
29	Cruise/Acceleration	$24 \le VSP_i < 30$	$25 \le v_i < 50$	
30	Cruise/Acceleration	$30 \le VSP_i$	$25 \le v_i < 50$	
33	Cruise/Acceleration	$VSP_i < 6$	$50 \le v_i$	
35	Cruise/Acceleration	$6 \le VSP_i < 12$	$50 \le v_i$	
37	Cruise/Acceleration	$12 \le VSP_i < 18$	$50 \le v_i$	
38	Cruise/Acceleration	$18 \le VSP_i < 24$	$50 \le v_i$	
39	Cruise/Acceleration	$24 \le VSP_i < 30$	$50 \le v_i$	
40	Cruise/Acceleration	$30 \le VSP_i$	$50 \le v_i$	

The low signal-to-noise ratio in the VSP calculations—particularly for the speed and acceleration derivation—leads to uncertainty in the operating mode assignment and distribution. In addition, the alternative VSP calculation from torque and RPM peaks well beyond the highest bin of 30 kW/metric ton in these CARMA tests. Despite criticism that MOVES VSP bins are too broad, and should be more narrowly defined like in the Comprehensive Modal Emissions Model (CMEM),(*30*) measurement noisiness leads to VSP assignments and distributions that may not be representative of CACC or ACC driving behavior. Considering that emission rates correlate well with operating modes (*29*), the current VSP bin structure in MOVES may be causing an under-prediction in energy and emission results.

Interestingly, driving behavior changes between the ACC and CACC runs are more clearly distinguished when VSP is derived from torque and RPM than when it is derived from speed and acceleration. These following behavior differences are well depicted in Figure 5, such that the operating mode distribution with $VSP(\tau, n_{RPM})$ skewed towards high speed and high power bins. We also find that there is fairly good agreement between the time fractions spent in each operating mode in the representative ACC and CACC run for reference $VSP(v, a)$ and alternative $VSP(\tau, n_{RPM})$ respectively. The starker contrast is between the VSP calculation methods than the following technology.

Figure 5. Operating mode distributions using reference $VSP(v, a)$ (top) and alternative $VSP(\tau, RPM)$ (bottom) for representative runs CACC 9 and ACC 1558.

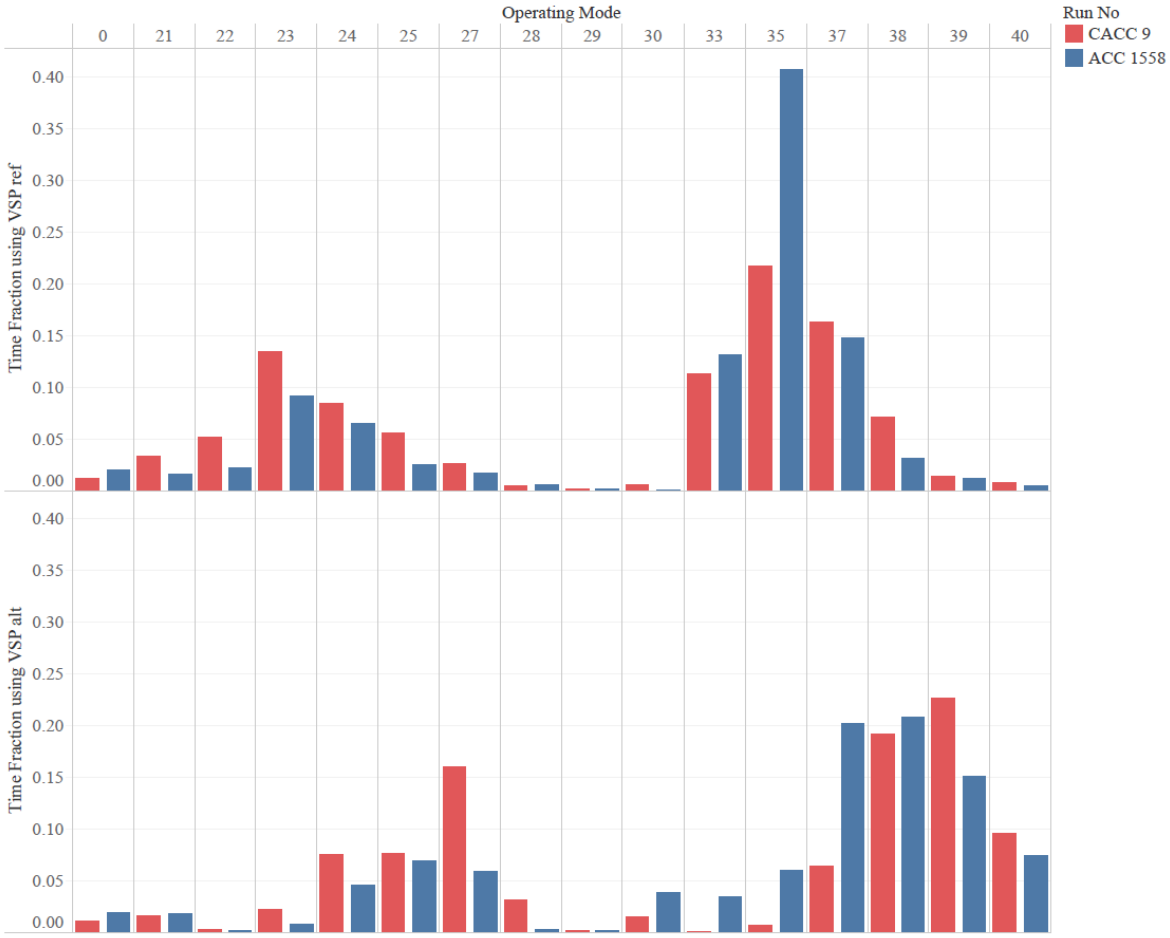

With the operating mode distributions by run, we were finally able to compare energy consumption and emissions using MOVES. Each run was defined as a separate restricted-access highway link (roadTypeID 2) and the operating mode distributions were used as project-level inputs to MOVES. To match the CARMA testing as best as possible, we also entered the average platoon speed and distance traveled of the lead vehicle for every run as MOVES inputs. Since all the CARMA SRXs had odometer readings well under 30,000 miles, we assumed they were new vehicles without any deterioration to their emission after-treatment systems. National defaults were applied for all the other project-level MOVES inputs.

Depending on VSP method, the energy and emission results varied greatly. We normalized the MOVES emission inventories by the miles traveled in order to fairly compare between runs using distance-based emission rates (in grams per mile). Figure 6 presents emission rates for nitrogen oxides (NOx) and fine particulate matter (PM2.5) as well as total energy consumption rates according to the two VSP methods. What jumps out between the methods is that the alternative $VSP(\tau, n_{RPM})$ generates energy rates that are roughly twice, PM2.5 rates that are 2-3 times, and NOx rates that are 3-4 times as large as the reference $VSP(v, a)$. Given the issues with when using the measured speed and acceleration to calculate VSP and assign operating modes, it is likely that $VSP(v, a)$ is underpredicting emissions and energy consumption for CARMA.

The rates based on reference $VSP(v, a)$ are more or less consistent between runs for NOx, PM2.5, and energy consumption. On the other hand, the rates from alternative $VSP(\tau, n_{RPM})$ do reflect some greater variability, which is more in line with the behavioral differences for ACC and CACC described above, although it is difficult to draw any conclusions. For $VSP(\tau, n_{RPM})$, energy and NOx rates between the ACC and CACC runs are mostly a wash. Due to large discrepancy in the PM2.5 rates for ACC Runs 1546 and 1558, those results are also inconclusive.

Figure 6. (a) Emission rates for NOx, PM2.5, and energy rates by run using alternative $VSP(\tau, n_{RPM})$ from MOVES, and (b) emission rates for NOx, PM2.5, and energy rates by run using alternative $VSP(v, a)$.

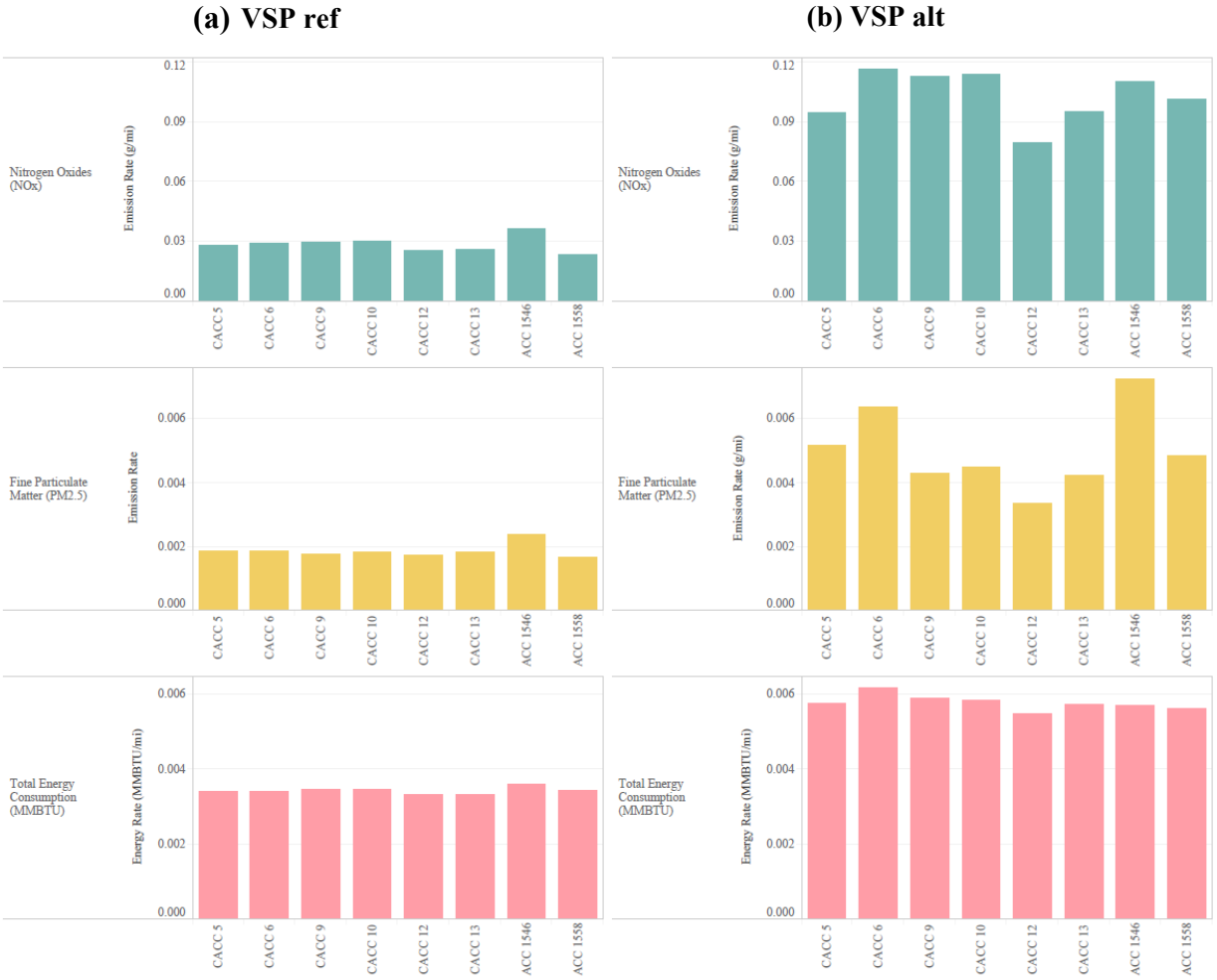

SUMMARY

Results from the CARMA tests challenge some of the projected benefits of ACC- and CACC-following technologies while confirming some others. Our analysis shows that the ACC platoons were more likely to experience oscillations before reaching a cruising speed than CACC, which aligns well with other literature. Many CACC studies—CARMA included—have tried to configure their vehicle control algorithms to close the following time gaps as quickly as possible, but this has resulted in more vehicle jerk.

We found that the relaxed ACC-following behavior exhibited in the CARMA tests may lead to a less aggressive driving trace and improved user comfort. Most of the CACC runs in CARMA converged to a specific time gap of around one second and stabilized at the cruising speeds, whereas the ACC runs have comparable average time gaps but did not stabilize. One of the most common modeling assumptions is that CACC systems will reduced time gaps over ACC, but this

CARMA analysis could not confirm these time gap reductions. We also examined the comparability of CARMA runs through the kinetic intensity ratio. Despite using the same general test procedure of switching between 45-mph and 60-mph cruising periods, there was some definite variability from run to run. The professional drivers may also introduce some bias in terms of close vehicle following compared to real-world conditions with untrained drivers.

In the absence of tailpipe emission and energy consumption measurements, estimates can be modeled. This paper presented two methods for calculating vehicle-specific power, which is later used to develop MOVES operating mode distributions and then emission and energy estimates. More commonly VSP is derived from speed and acceleration, but this method produced substantial noise with the CARMA instrumented vehicle data regardless of following technology. In this analysis of energy and emission impacts, the VSP derived from axle torque and engine RPM generated much cleaner, more resolved results. Therefore, instantaneous torque and RPM measurements are much preferred for the VSP calculation in this analysis of CARMA test data.

Even still, the noisiness in calculated VSP makes it difficult to properly assign values to MOVES VSP bins in an effort to effectively model ACC and CACC behavior. Furthermore, the highest MOVES VSP bin is for 30 kW/metric ton or more, but many of the CARMA tests showed instantaneous spikes in VSP based on torque and RPM that were up to 12 times greater than that highest bin. As an artifact of noise and outliers, energy, NOx, and PM2.5 impacts were muddled when using either VSP method. Researchers should ensure the data quality of the VSP time series before proceeding to emissions and energy modeling. Collectively these findings suggest the structuring of the power bins is critical to the evaluation of ACC and CACC tests, and imply that finer bins may be necessary to accurately assess differences between these following technologies. In addition, real-time portable emissions and fuel consumption monitoring is needed to validate any modeled benefits of these testing scenarios.

Based on this analysis of the CARMA data, we have compiled a few other recommendations for future testing. First, better consistency of drive cycles and kinetic intensity across runs would enhance comparability. In previous modeling studies, we compared driving with ACC and CACC systems against a baseline of naturalistic driving to calculate benefits. Both ACC Runs 1546 and 1558 were missing some key data for following vehicles and often had conflicting results. This suggests additional benchmarking of manual and ACC driving is needed.

While the Cadillac SRX test fleet performed admirably, each manufacturer produces different ACC controls, which can vary depending on the intended vehicle type and driver. It would be worthwhile to test a diverse set of commercially available ACC technologies with and without V2V communications. Similarly, it would be useful to recalibrate and test these CACC APF control algorithms for optimal user comfort, fuel efficiency, and/or air quality benefits. Further testing of these following technologies under different conditions and optimizations would improve our understanding of the interplay between operational and environmental benefits.

ACKNOWLEDGMENTS

We wish to thank Kevin Dopart from the Intelligent Transportation System Joint Program Office (ITS JPO) for continuing to sponsor research on the impact of connected and automated vehicles. We also thank Taylor Lochrane from FHWA's Turner-Fairbank Highway Research Center for designing and overseeing the Cooperative Automation Research Mobility Applications (CARMA) Program that provided data for this study. Lastly, we appreciate the thoughtful review and recommendations by our many Volpe colleagues and external collaborators.

REFERENCES

1. International Standard, I.-20035 (2019). Intelligent Transport Systems — Cooperative Adaptive Cruise Control Systems (CACC) — Performance Requirements and Test Procedures. 2019.
2. Tian, D., G. Wu, K. Boriboonsomsin, and M. J. Barth. Performance Measurement Evaluation Framework and Co-Benefit / Tradeoff Analysis for Connected and Automated Vehicles (CAV) Applications: A Survey. National Center for Sustainable Transportation, 2017.
3. FHWA. CARMA Overview | FHWA. https://highways.dot.gov/research/research-programs/operations/CARMA. Accessed Jul. 24, 2019.
4. Tiernan, T. A., N. Richardson, P. Azeredo, W. G. Najm, and T. Lochrane. Test and Evaluation of Vehicle Platooning Proof-of-Concept Based on Cooperative Adaptive Cruise Control. Volpe Center, 2017, p. 129.
5. Tiernan, T., P. Bujanovic, P. Azeredo, W. Najm, and T. Lochrane. CARMA Testing and Evaluation of Research Mobility Applications. Publication DOT-VNTSC-FHWA-19-15. FHWA, 2019, p. 61.
6. Bujanovic, P. Developing Vehicle Platoons and Predicting Their Impacts. University of Texas at Austin, Austin, Texas, 2018.
7. SAE. Taxonomy and Definitions for Terms Related to Driving Automation Systems for On-Road Motor Vehicles (J3016).
8. Eilbert, A., I. Berg, and S. Smith. Systematic Review and Meta-Analysis of Adaptive Cruise Control Applications: Operational and Environmental Benefits. In 2019 TRB Annual Meeting, No. 19–04981, Washington, D.C., 2019.
9. Bu, F., H.-S. Tan, and J. Huang. Design and Field Testing of a Cooperative Adaptive Cruise Control System. Presented at the American Control Conference, 2010.
10. Nowakowski, C., S. E. Shladover, D. Cody, F. Bu, J. O'Connell, J. Spring, S. Dickey, and D. Nelson. Cooperative Adaptive Cruise Control: Testing Drivers' Choices of Following Distances. Publication UCB-ITS-PRR-2011-01. California PATH Program, Institute of Transportation Studies, University of California at Berkeley, 2011.
11. Milanes, V., S. E. Shladover, J. Spring, C. Nowakowski, H. Kawazoe, and M. Nakamura. Cooperative Adaptive Cruise Control in Real Traffic Situations. IEEE Transactions on Intelligent Transportation Systems, Vol. 15, No. 1, 2014, pp. 296–305. https://doi.org/10.1109/TITS.2013.2278494.
12. Milanés, V., and S. E. Shladover. Modeling Cooperative and Autonomous Adaptive Cruise Control Dynamic Responses Using Experimental Data. Transportation Research Part C: Emerging Technologies, Vol. 48, 2014, pp. 285–300. https://doi.org/10.1016/j.trc.2014.09.001.
13. Eilbert, A., G. Noel, L. Jackson, I. Sherriff, and S. B. Smith. A Framework for Evaluating Energy and Emission Impacts of Connected and Automated Vehicles through Traffic Microsimulations. Presented at the 97th Annual Meeting of the Transportation Research Board, 2018.

14. Mattas, K., M. Makridis, C. Thiel, M. Alonso Raposo, T. Toledo, B. Ciuffo, C. Fiori, and G. Fontaras. Analyzing the Impact of Cooperative Adaptive Cruise Control Systems on Traffic Flow and Energy Consumption in a Real Freeway Scenario. Presented at the 97th Annual Meeting of the Transportation Research Board, 2018.
15. Wang, Z., G. Wu, P. Hao, K. Boriboonsomsin, and M. Barth. Developing a Platoon-Wide Eco-Cooperative Adaptive Cruise Control (CACC) System. Presented at the 2017 IEEE Intelligent Vehicles Symposium (IV), 2017.
16. Mamouei, M., I. Kaparias, and G. Halikias. A Framework for User- and System-Oriented Optimisation of Fuel Efficiency and Traffic Flow in Adaptive Cruise Control. Transportation Research Part C: Emerging Technologies, Vol. 92, 2018, pp. 27–41. https://doi.org/10.1016/j.trc.2018.02.002.
17. Ma, J., J. Hu, E. Leslie, F. Zhou, and Z. Huang. Eco-Drive Experiment on Rolling Terrain for Fuel Consumption Optimization – Summary Report. Publication FHWA-HRT-18-037. Leidos, Inc., 2018.
18. Knoop, V. L., M. Wang, I. Wilmink, D. M. Hoedemaeker, M. Maaskant, and E.-J. Van der Meer. Platoon of SAE Level-2 Automated Vehicles on Public Roads: Setup, Traffic Interactions, and Stability. Transportation Research Record: Journal of the Transportation Research Board, 2019, p. 036119811984588. https://doi.org/10.1177/0361198119845885.
19. FHWA. Cooperative Automated Research Mobility Applications (CARMA) 2 | Department of Transportation - Data Portal. https://data.transportation.gov/Automobiles/Cooperative-Automated-Research-Mobility-Applicatio/dusd-cr84. Accessed Jul. 24, 2019.
20. Elert, G. Kinematics & Calculus. The Physics Hypertextbook. https://physics.info/kinematics-calculus/. Accessed Jul. 28, 2019.
21. University of Idaho. Traffic Flow Parameters. https://www.webpages.uidaho.edu/niatt_labmanual/Chapters/trafficflowtheory/theoryandconcepts/TrafficFlowParameters.htm. Accessed Jul. 28, 2019.
22. O'Keefe, M. P., A. Simpson, K. J. Kelly, and D. S. Pedersen. Duty Cycle Characterization and Evaluation Towards Heavy Hybrid Vehicle Applications. Presented at the SAE World Congress & Exhibition, 2007.
23. US EPA, O. MOVES and Other Mobile Source Emissions Models. US EPA. https://www.epa.gov/moves. Accessed Jul. 28, 2019.
24. Cadillac Pressroom - United States - SRX. media.gm.com. https://media.gm.com/content/media/us/en/cadillac/vehicles/srx/2013.tab1.html. Accessed Jul. 29, 2019.
25. Angular Motion - Power and Torque. https://www.engineeringtoolbox.com/angular-velocity-acceleration-power-torque-d_1397.html. Accessed Jul. 29, 2019.
26. Exhaust Emission Rates for Light-Duty On-Road Vehicles in MOVES2014. Publication EPA-420-R-15-005. Environmental Protection Agency, 2015.

KEYWORDS

Adaptive cruise control, cooperative automation, ACC, CACC, all predecessor following, APF, platoon, vehicle-to-vehicle communications, V2V, time gap, user comfort, fuel savings, emission reductions